Neuroinflammation in obesity investigated with positron emission tomography and post-mortem human biopsies

Eleni Rebelos[1,2,3*], Senthil Palani[1,2], Miikka-Juhani Honka[1,2], Jouni Tuisku[1], Laura Pekkarinen[1], Aino Latva-Rasku[1,2], Laura Ekblad[1], Ekaterina Saukko[4], Richard Aarnio[1], Jussi Hirvonen, Simo Salo[1], Johan Rajander[4], Maria Gardberg[5] Saila Kauhanen[6], Mika Helmiö[6], Paulina Salminen[6,7], Christos S. Mantzoros[8], Juha Rinne[1,9], Lauri Nummenmaa[1,10], Anne Roivainen[1,2], Pirjo Nuutila[1,2,8]

Brain ^{11}C-PK11195 uptake and obesity

[1] Turku PET Centre, University of Turku, Åbo Akademi University and Turku University Hospital, Turku, Finland

[2]InFLAMES Research Flagship Center, University of Turku, Turku, Finland

[3] Department of Clinical and Experimental Medicine, University of Pisa, Pisa, Italy

[4]Department of Diagnostic Radiology, University of Turku and Turku University Hospital, Turku, Finland

[5] Institute of Biomedicine, University of Turku and TYKS Laboratories, Department of Pathology, Turku University Hospital, Turku, Finland

[6]Division of Digestive Surgery and Urology, Turku University Hospital, P.O. Box 52, FIN-20521, Turku, Finland.

[7]Department of Surgery, University of Turku, Turku, Finland

[8]Department of Medicine, Beth Israel Deaconess Medical Center, Harvard Medical School, Boston, MA, 02215, USA; Department of Medicine, Boston VA Healthcare System, Harvard Medical School, Boston, MA, 02215, USA.

[6] Department of Neurology, Turku University Hospital, Turku, Finland

[7] Department of Psychology, University of Turku, Turku, Finland

[8]Department of Endocrinology, Turku University Hospital, Turku, Finland

**Corresponding author*: Eleni Rebelos, MD, PhD, email: eleni.rebelos@utu.fi

Word Count Abstract:
Word Count Main Text:
Number of References:
Number of Tables:
Number of Figures:
ClinicalTrials.gov Identifier: **NCT04343469**

Abstract

Obesity is characterized by a chronic, low-grade peripheral inflammation, but whether similar inflammatory processes occur in the brain remains unclear. In human brain biopsies from donors with obesity and lean controls, we observed histological evidence of increased macrophage-related inflammation in white matter in the obesity group. In contrast, in vivo imaging with the translocator protein (TSPO) tracer ^{11}C-PK11195 revealed higher uptake in healthy lean individuals compared with patients with obesity. To clarify this apparent discrepancy, we performed double immunostaining for TSPO with CD68 or CD31. These analyses showed greater TSPO/CD31 co-localization in lean donors than in those with obesity, whereas TSPO/CD68 co-localization did not differ between groups. Together, these findings provide the first pathological evidence of white-matter neuroinflammation in human obesity and suggest that, in healthy individuals, ^{11}C-PK11195 uptake may predominantly reflect endothelial TSPO expression.

Keywords: positron emission tomography, TSPO, brain inflammation, obesity

Abbreviations: BGU, brain glucose uptake; BMI, body mass index; CBF, cerebral blood flow; CI, confidence interval; CNS, central nervous system; CRP, C-reactive protein; FDG, [^{18}F]-fluorodeoxyglucose; FDR, false discovery rate; FFA: free fatty acids; FFM: fat-free mass; FUR, fractional uptake rate; IGT: impaired glucose tolerance; MNI, Montreal Neurological Institute; NGT: normal glucose tolerance; OGTT, oral glucose tolerance test; PET, positron emission tomography; SPM, statistical parametric mapping**;** T2D, type 2 diabetes

Introduction

Obesity is characterized by chronic low-grade peripheral inflammation(1). In recent years, interest has grown in whether similar inflammatory processes also occur in the brain in the context of obesity(2). Preclinical studies in mice and diet-induced obesity (DIO) rats have shown that shortly after initiation of a high-fat diet, both microglia—the resident macrophages of the CNS—and astrocytes become activated and proliferate(3). Notably, this response emerges before measurable weight gain and appears to be centrally driven by neuronal stress rather than secondary to peripheral inflammation. Gliosis may therefore represent an early, transient protective mechanism; however, if high-fat feeding and obesity persist, neuroinflammation becomes chronic(3). Neuroinflammation is increasingly recognized as a key mechanism contributing not only to disturbances in energy homeostasis and glucose metabolism(2) but also to cognitive decline(4,5)—a condition for which both obesity and diabetes are independent risk factors(6,7).

In humans, indirect evidence of obesity-related neuroinflammation was first proposed by Thaler et al., who reported that the T2-weighted MRI hyperintensity in the left hypothalamus/amygdala correlated directly with BMI, and proposed this as a sign of gliosis (3). As acknowledged by the authors, this hyperintensity signal is not specific to neuroinflammation, as similar MRI findings can arise from edema, infection, or tumors(3). In our own earlier work, we were unable to replicate the association with BMI, and we observed only moderate inter-rater reliability between two independent, blinded neuroradiologists(8). Subsequent MRI-based studies using a quantitative MRI technique to measure T2 relaxation time in the medio-basal hypothalamus (MBH) have also suggested possible neuroinflammation in MBH in obesity(9), and interestingly the T2 relaxation time in the MBH has been associated with glial fibrillary acidic protein (GFAP) content in both animals and humans(9,10). However, given the very small size of the hypothalamus and its

susceptibility to partial-volume effects, MRI-based gliosis in this region must be interpreted with caution. More broadly, conventional MRI lacks the cellular specificity required to distinguish inflammation from other structural or metabolic alterations. Moreover, although hypothalamic inflammation has been a topic of intense research, it is not clear if obesity-induced inflammation would be restricted only in that region.

Taken together, current evidence leaves unresolved the fundamental question of whether human obesity is associated with brain inflammation and in which brain areas. The primary aim of the present study was therefore to address this question directly by combining with molecular imaging using ^{11}C-PK11195 PET in patients with obesity and healthy controls, enabling assessment of brain inflammation at the whole-brain level and *ex vivo* histological analyses of human brain tissue from donors with obesity and lean donors. Additional immunohistochemical analyses were performed on the brain biopsies in order to help elucidate the clinical molecular imaging data.

Secondary aim of the study, was to explore associations of variables of brain inflammation assessed herein with neurocognitive testing outcomes, obesity, insulin resistance and circulating systemic and centrally-derived inflammatory markers given prior hypotheses linking brain inflammation with neurocognitive decline and insulin resistance, circulating markers of inflammation systemically.

We and others have consistently shown in previous work that patients with obesity exhibit higher brain glucose uptake (BGU) than healthy controls during insulin clamp experiments(11–13). The mechanisms underlying this enhanced BGU remain unclear. One plausible explanation is that widespread neuroinflammation—particularly astrocytic activation—could increase glucose utilization, consistent with the fact that astrocytes and microglia represent the most abundant cells in the brain and recent evidence that in the brain

glucose is predominantly metabolized by astrocytes through the astrocyte–neuron lactate shuttle (ANLS)(14). Thus, if obesity were associated with diffuse brain inflammation, this could provide a mechanistic link to the elevated BGU observed in humans *in vivo*. Tertiary aim of the study, was thus to provide mechanistic insight into our earlier observations of increased BGU in obesity.

Research Design and Method

Study population The study cohort consisted of 24 subjects with severe obesity consecutively recruited in the Division of Digestive Surgery of Turku University Hospital in the years 2019-2020 and candidates for metabolic bariatric surgery (MBS). 19 healthy lean healthy subjects, recruited on a volunteer basis via advertisements at the local newspapers served as controls. None had any clinical diagnosis of neurological disease. From the subjects affected by obesity, 4 had type 2 diabetes (T2D) and 11 had either impaired glucose tolerance or impaired fasting glucose, according to the ADA criteria(15). Patients with T2D used either metformin (1-3 g daily), or a combination of metformin and SGLT2-inhibitors. Patients on insulin treatment were excluded. All subjects underwent a screening visit before inclusion in the study, during which a standard (75 g) oral glucose tolerance test was performed. Metformin was withheld 48 h and SGLT2 inhibitors 24 h before the metabolic studies. Prior to inclusion, each participant gave written informed consent. Each study protocol included in this study was approved by the Ethics Committee of the Hospital District of Southwest Finland and conducted in accordance with the Declaration of Helsinki. The study was registered in Clinicaltrials.gov (ClinicalTrials.gov Identifier: **NCT04343469**). The anthropometric and metabolic characteristics of all study participants are listed in **Table 1.**

[^{18}F]-FDG studies performed under euglycemic hyperinsulinemic clamp and ^{11}C-PK11195 studies The euglycemic hyperinsulinemic clamp was performed as previously described(16,17). In brief, a primed, continuous infusion of insulin (Actrapid; Novo Nordisk, Copenhagen, Denmark) was given at a rate of 40mU·m^{-2}·min^{-1}. During the clamp, a variable rate 20% glucose solution was infused to maintain euglycemia at 5 mmol/L. Plasma glucose levels were measured every 5–10 min throughout the clamp. During the clamp, samples for plasma insulin and serum FFA measurement were taken at baseline and at 30 and 60 min, respectively, thereafter. At 77±15 min into the clamp, subjects were positioned in a GE Discovery 690 PET/CT scanner (General Electric Medical Systems, Milwaukee, WI, USA) and [^{18}F]FDG (181±10 MBq) was injected intravenously over 15 s. The acquisition of brain radioactivity started 76 ± 20 min after [^{18}F]FDG injection. On a separate day, participants returned to the facilities of Turku PET Centre after an overnight fast. ^{11}C-PK11195 PET imaging was performed with the same PET scanner (GE Discovery 690 PET/CT scanner, General Electric Medical Systems, Milwaukee, WI, USA). The subjects were injected intravenously with ^{11}C-PK11195 (500±9 MBq) over 15 s and the brain was scanned for 60 min. To obtain anatomic reference for PET data region of interest (ROI) analysis and to be able to exclude potential anatomical abnormalities, the subjects underwent MRI with a 3T PET-MRI scanner (Philips Ingenuity TF PET-MR device, Philips Healthcare, the Netherlands). In a minority of subjects (N=12), blood samples were also drawn to measure circulating ^{11}C-PK11195 metabolites.

Image processing PET and MRI data were processed using the MAGIA pipeline in SPM12 software (Welcome Trust Centre for Neuroimaging, London, UK) MATLAB (The Mathworks, Natick, MA), in which PET images were realigned and co-registered to individual T1-weighted MR images using SPM12 software (Welcome Trust Centre for Neuroimaging, London, UK)(18). Cortical lobes along with subcortical brain ROIs were parcellated from T1

MRI data using FreeSurfer software (version 5.3.0, http://freesurfer.net/), after which the corresponding regional PET time activity curves (TAC)s were created. As nonfocal brain inflammation was expected, TACs from three large cerebral ROIs (cortical gray matter (GM), cortical white matter (WM) and combined GM and WM) were calculated as a volume weighted average of the partial volume corrected TACs.

^{11}C-PK11195 modelling Distribution volume ratios (DVR) using Logan's method within 20-60 min, with respect to pseudoreference region using supervised clustering analysis (SCA), were calculated in order to obtain an estimate for the specific [^{11}C]PK11195 binding(19). For an exploratory voxel-level analysis, parametric binding potential (BP_{ND}) images were calculated using a basis function implementation of simplified reference tissue model with 250 basis functions. The resulting parametric maps were further normalized into MNI152 space in SPM12 and smoothed with Gaussian 8mm FWHM filter.

[^{18}F]FDG modelling BGU data were modelled using fractional uptake rate as previously described(20). Thus, BGU (in $\mu mol \cdot 100g^{-1} \cdot min^{-1}$) was calculated at the voxel level as fractional uptake rate multiplied by the average plasma glucose concentration from the injection until the end of the brain scan, divided by the lumped constant for the brain (set at 0.65)(21).

Calculation of Insulin-Stimulated Glucose Disposal (M Value) The M value was calculated as a measure of whole-body insulin sensitivity, as previously described(20), and expressed per kilogram of fat-free mass ($\mu mol \cdot kg_{FFM}^{-1} \cdot min^{-1}$), because this normalization minimizes differences due to sex, age, and body weight(22).

Cognitive function testing Neuropsychological function was assessed by an online survey using Gorilla Experiment Builder (gorilla.sc) platform(23). The survey consisted of several tasks that measure working memory (N-back tasks with N = 1 and N = 2, digit span text entry), memory encoding and retrieval with CERAD Word List Memory task type test, vigilance,

simple reaction time, and fluid intelligence with the matrix reasoning item bank (MaRs-IB)(24) which is a modified open-source variant of the Raven's progressive matrices test. Emotional sensitivity was measured by asking subjects to report their feelings of valence (pleasure-displeasure) and arousal to a set of pleasant, unpleasant and neutral pictures derived from the International Affective Picture system (IAPS)(25). The survey was performed in a quiet room using a standard desktop computer, under the supervision of a trained nurse.

Analytical methods Plasma glucose was measured in duplicate using the glucose oxidase technique (Analox GM7 or GM9, Analox Instruments Ltd., London, UK). Glycosylated hemoglobin (HbA_{1c}) was measured by high- performance liquid chromatography (Variant II Haemoglobin A_{1c}, Bio-Rad Laboratories, CA, USA). Plasma insulin was determined by time-resolved immunofluorometric assay (AutoDELFIA, Perkin Elmer Life and Analytical Sciences). Serum FFA were measured with a photometric enzymatic assay (FFA-HR(2),Wako Chemicals GmbH, Neuss, Germany) on Modular P800 automatic analyzer (Roche Diagnostics, Mannheim, Germany). Serum adiponectin, TNF-α, IL-6, IL-8, NGF, leptin and Plasminogen activator inhibitor 1 (PAI-1) were measured using HADCYMAG-61K panel (Merck/Millipore). Serum NfL and GFAP concentrations were analyzed by the Biomarkers for Neurodegenerative Disorders research group at the University of Eastern Finland (Kuopio, Finland; https://www3.uef.fi/fi/web/neuro/biomarkers (www3.uef.fi in Bing)) using the single-molecule array (SIMOA) platform (Quanterix Corporation, Billerica, MA, USA). NfL was measured with the "Advantage" kit and GFAP with the "Discovery" kit.

Post-mortem human biopsies Paraffin embedded human brain biopsies were obtained from Auria bio-bank, from five lean and six subjects with obesity. Donors were matched for age (range from 15 to 48 years) and sex (4 women and 7 men) and did not have any brain diseases.

Immunohistochemistry *6* μm human brain biopsies sections were used to examine the percentage of CD68 positive macrophages, TSPO and Mitok (a Mitochondrial marker). The sections were incubated with an anti-human CD68 antibody (1: 100; catalog number: M0876, Dako Agilent, Santa clara, United States) and an anti-human TSPO (1: 1000; catalog number: Ab109497, Abcam, Cambridge, United Kingdom), and anti-human MITOK antibody (catalog number: MU213-UC, BioGenex, Arnhem, The Netherlands), followed by development of a color reaction using 3.3′-diaminobenzidine (Bright-DAB, BS04-110; ImmunoLogic, Duiven, the Netherlands). The stained slides were scanned with a digital slide scanner (Pannoramic 250 Flash; 3DHISTECH, Ltd., Budapest, Hungary) then images were processed and analyzed with GIMP and Image J.

Immunofluorescence Double staining on *6* μm human brain biopsies sections were performed to investigate the percentage of TSPO in endothelial cells (CD31, a endothelial cell marker) and percentage of TSPO in macrophages (CD68, a macrophage marker). The sections were stained with mouse anti-human CD68 (1: 200; catalog number: M0876, Dako Agilent, Santa clara, United States) and Rabbit anti-human TSPO antibody (1: 1000; catalog number: Ab109497, Abcam, Cambridge, United Kingdom) or mouse anti-human CD31 antibody (1: 100; catalog number: M0823, Dako Agilent, Santa clara, United States) and anti-human TSPO antibody, followed by goat anti-Mouse Alexa Fluor 594 conjugated secondary antibody (1:1000; catalog number: A-11032, Invitrogen, ThermoFisher Scientific, Waltham, United States) and donkey anti-Rabbit Alexa Fluor 488 conjugated secondary antibody (1:1000; catalog number: A-21206, Invitrogen, ThermoFisher Scientific, Waltham, United States). Then the sections were mounted with ProLong Gold antifade with DAPI (catalog number: P36931, Invitrogen, ThermoFisher Scientific, Waltham, United States). The stained slides were finally scanned with a digital slide scanner (Pannoramic Midi fluorescence slide scanner; 3DHISTECH, Ltd., Budapest, Hungary).

Image processing workflow The original raw data MIRAX from whole-slide double stained brain tissue section image format was converted to OME-Zarr chunked multi-dimensional arrays to facilitate image processing. Tissue section boundaries were generated using global thresholding of the red channel (corresponding to either CD68, a macrophage marker or CD31, an endothelial cell marker), with the resulting binary raster mask then vectorized into polygon coordinates and stored as text files. The raw whole-slide image data contained imaging artifacts that needed to be excluded from the analysis. For this, a global threshold value was used to create a binary mask of the artifacts, which was subsequently converted into vector coordinates. Channel-based analysis was then performed only on the data that fell within the tissue and outside of the artifact boundaries. A StarDist model using pre-trained weights was used to detect nuclei in the DAPI channel. The centroid of each detected nucleus was used to draw a circular area with a radius of 120 pixels. The overlap coefficients of the red (CD68, Macrophages or CD31, Endothelial cells), and green channels (corresponds to TSPO expression) contained within the circles were measured. The image processing pipeline was created using Python scripts with the end-to-end automation orchestrated using Nextflow. The full data processing was performed on supercomputing resources provided by the Centre for Scientific Computing.

Statistical analysis Data are presented as mean ± SD (or median [interquartile range IQR] for non-normally distributed variables). Voxel-level two sample t-test analysis was performed with statistical parametric mapping (SPM) (SPM12 toolbox for Matlab). Before the voxel-level analysis, the BP_{ND} images were smoothed in SPM12 with Gaussian 8mm FWHM filter to compensate for anatomical variability in image normalization and to improve signal-to-noise ratio. The cluster level correction for multiple comparisons was performed using false discovery rate (FDR) with significance level of $p<0.05$. Linear regressions were performed in SPM to evaluate correlations between BGU and [^{11}C]PK11195 uptake and single regressors

(BMI, M value, CRP etc.) while controlling for confounding factors (in the SPM contrast, the controlling variables were set to a value of 0). Glucose and [^{11}C]PK11195 uptake values were extracted from the global ROI with Marsbar plug-in for Matlab and visualized with the single regressors using scatter-plot correlation coefficients (r). Further statistical analyses were done using JMP version 13.0 (SAS Institute, Cary, NC, USA). A p value < 0.05 was considered statistically significant.

Results

Baseline characteristics of the clinical study

The two groups were well-matched in terms of age and gender. As expected, subjects with obesity had higher BMI (and other measures of adiposity), worse insulin sensitivity as indexed by the M value and the OGIS and higher circulating hs-CRP values, compared to the lean individuals. Plasma leptin, and TNF-α, were also higher in subjects with obesity and were suggestive of low-grade systemic inflammation. PAI-1 levels were almost double in patients with obesity, whereas there was no statistical difference in brain-derived markers of neurofilament light chain (NfL) and GFAP (**Table 1**).

Of the battery of cognitive function evaluated, we found that patients with obesity performed worse in the memory, and fluid intelligence test compared to the healthy controls (**Table 2**), in line with previous studies(26–29). Fluid intelligence refers to the ability to reason and solve problems without relying on pre-existing knowledge, which is also referred to as “crystallized intelligence”. When accounting for age and education level the difference in memory remained significant, whereas for fluid intelligence there was only a tendency of better performance in the healthy lean controls. There were no significant differences in reaction times between the two groups.

In line with previous findings from us and others, subjects with obesity had higher BGU during insulin clamp than the lean controls, and in the whole dataset, BGU correlated inversely with the M value (**Supplementary Figure 1**).

Brain inflammation assessed with imaging and post-mortem human brain tissue sections

To investigate whether human obesity is associated with brain inflammation, we conducted ^{11}C-PK11195 PET imaging under fasting conditions. This tracer has previously been used to detect brain inflammation in diseases such as multiple sclerosis. We hypothesized that, if obesity were accompanied by brain inflammation, individuals with obesity would exhibit higher ^{11}C-PK11195 uptake than healthy lean controls. Contrary to this expectation, ^{11}C-PK11195 uptake was higher in lean participants compared with those with obesity within white matter at the whole-brain level, while no group differences were observed in cortical regions (**Figure 1**). In cross-sectional analyses, ^{11}C-PK11195 uptake correlated negatively with BMI in overlapping brain areas (**Figure 2**). ^{11}C-PK11195 uptake correlated negatively with hs-CRP; this correlation was found at the white matter at the whole-brain level. When accounting for BMI the correlation between ^{11}C-PK11195 uptake and hs-CRP remained significant but it was restricted in frontal regions (**Supplementary Figure 2**).

To further explore our primary hypothesis, whether there is evidence of brain inflammation in obesity and to put it in context with our clinical findings, we performed immunostaining of human brain biopsies using CD68, a macrophage marker. Immunohistochemistry analysis showed that donors who had obesity had significantly higher percentage area of CD68 positive macrophages compared to lean subjects (0.63 [0.50-0.73] *vs* 0.34 [0.21-0.44] % respectively, p=0.02), indicative of inflammatory insult in the context of obesity (**Figure 3C**).

^{11}C-PK11195 uptake and TSPO as a possible marker of endothelial function

In order to try to elucidate our clinical findings we further performed immunostainings of the available brain biopsies. As TSPO is a mitochondrial membrane protein and it has been also linked with endothelia(30), our secondary hypotheses were that the higher ^{11}C-PK11195 uptake observed in lean subjects could be due to better mitochondrial density, or better endothelial function.

There were no differences in TSPO and mitochondrial staining between brain biopsies from lean donors and donors with obesity (**Figure 3 A-C**). Moreover, we observed that Mitok staining was widely distributed throughout the tissue without defining any specific cell types in our immunostainings. Therefore, we did not include Mitok in our double stainings with TSPO.

To refine our assessment of TSPO expression, we focused on major brain cell populations known to express TSPO and participate in neuroinflammatory processes. Because TSPO is expressed predominantly in macrophages and endothelial cells, we selected CD68 and CD31 as markers for these respective populations and performed double immunostaining with TSPO to enable cell-type–specific quantification. Image analysis using our processing workflow showed that TSPO expression tended to be higher in endothelial cells of lean compared with those with obesity (p=0.057) (**Figure 4C**). Consistent with this, co-localization of TSPO with endothelial cells was inversely associated with BMI (r=-0.62, p=0.04) (**Figure 4D**). In contrast, TSPO expression in macrophages (TSPO co-localization with CD68-positive cells) did not differ between groups (**Figure 4C**). These findings suggest that, in the context of obesity, the TSPO signal arises predominantly from endothelial cells. This pattern may lend support to the *in vivo* finding of increased ^{11}C-PK11195 uptake in healthy lean subjects

compared to patients with obesity. Moreover, supporting the interpretation that lean individuals may exhibit better endothelial function, in our clinical study ^{11}C-PK11195 uptake was inversely associated with PAI-1 levels (**Figure 2**). This relationship remained significant after adjusting for BMI (st. $\beta = -0.37$, $p = 0.03$). PAI-1 is a circulating marker closely linked to endothelial dysfunction(31).

Associations between ^{11}C-PK11195 uptake and clinical parameters

In the whole dataset ^{11}C-PK11195 uptake was directly related to the degree of insulin sensitivity (r=0.48, p=0.002). On the contrary, we could not detect any association between BGU and ^{11}C-PK11195 uptake. We did not detect any association between ^{11}C-PK11195 uptake and the markers of peripheral inflammation such as CRP, TNF-α, IL-6, MCP-1, NGF (data not shown), or with the brain-derived marker of neurofilament light chain (NfL).

Also, whereas patients with obesity had slightly numerically higher values of brain-derived marker of neurofilament light chain (NfL) and GFAP, these differences were not significant between groups and there was no relation with ^{11}C-PK11195 uptake (data not shown). Interestingly, with regards to cognitive function, ^{11}C-PK11195 uptake was inversely associated with the proportion of correct answers in vigilance test and in fluid intelligence in patients with obesity, whereas there was no such association in the lean group (**Figure 5**).

Discussion

The primary aim of this study was to determine whether human obesity is associated with brain inflammation. To address this question, we first conducted a clinical

PET study using ^{11}C-PK11195, a widely used first-generation TSPO radioligand for assessing neuroinflammation(32). Because the PET findings –in this cohort of subjects without neurological disease- were not straightforward, we complemented the imaging data with targeted analyses of human brain biopsies obtained from donors with obesity and lean controls. To our knowledge, this is the first study to assess brain inflammation in obesity using human brain tissue.

Contrary to our initial hypothesis, ^{11}C-PK11195 uptake was lower, not higher, in individuals with obesity compared with healthy lean controls. This finding aligns with contemporaneous reports from studies using either ^{11}C-PK11195(33) or second-generation TSPO tracers, all reporting higher TSPO uptake in lean individuals (34). If ^{11}C-PK11195 uptake reliably reflected neuroinflammation, this result would be counterintuitive. We thus examined brain tissue from five lean and six donors with obesity, matched for age and sex and without neurological disease. For the first time, we demonstrate increased macrophage infiltration in the white matter of donors with obesity, providing direct histological evidence of brain inflammation in human obesity. Although a previous study has also assessed presence of inflammation in human brain tissue from the MBH, that study only assessed GFAP levels and related them to the MRI signal, without performing a direct comparison in MBH inflammatory markers between donors with obesity and donors who had normal weight(9). Indeed, in that study, information regarding BMI of the human biopsy data was not even available(9). Thus, the increased astrocytosis in that study, may not have been necessarily related to obesity.

Having demonstrated brain inflammation in the white matter in obesity, a new clinical question arose: why do lean subjects exhibit higher ^{11}C-PK11195 uptake, selectively in white matter? TSPO is a highly hydrophobic protein with five transmembrane domains, primarily localized to the outer mitochondrial membrane. Given this localization, one

hypothesis is that higher TSPO uptake in lean subjects reflects better mitochondrial function. Alternatively, as TSPO expression in the normal brain is predominantly found in endothelial mitochondria(30), higher [^{11}C]PK11195 uptake in lean subjects could reflect superior endothelial function. To investigate these possibilities, we again analyzed the human brain tissue samples. We did not observe differences in mitochondrial number or total TSPO expression between donors with overweight or obesity and lean donors. We therefore performed double immunostaining of TSPO with either CD68 (a pan-macrophage marker) or CD31 (an endothelial marker). TSPO/CD68 co-localization did not differ between the groups, indicating similar TSPO expression within macrophages. In contrast, and to the best of our knowledge for the first time, we observed significantly higher TSPO/CD31 co-localization in lean donors compared with donors with overweight or obesity. Moreover, TSPO/CD31 co-localization was inversely associated with BMI. These findings suggest that the higher TSPO signal observed *in vivo* by PET in healthy lean subjects may be driven by greater endothelial TSPO expression. Further support for this interpretation comes from the inverse association between ^{11}C-PK11195 uptake and circulating PAI-1 levels. PAI-1 is released by damaged endothelial cells(31), but is also secreted by other tissues, including adipose tissue(35,36). The association between ^{11}C-PK11195 uptake and PAI-1 was stronger than that with BMI or hs-CRP and remained significant after adjustment for BMI, suggesting that circulating PAI-1 levels in this cohort more accurately reflect endothelial dysfunction. On the contrary, ^{11}C-PK11195 uptake did not associate with markers of systemic inflammation, such as TNF-α, IL-6, or IL-8, and it did not associate with the brain-derived markers NfL and GFAP. NfL is a novel biomarker reflecting neuroaxonal damage and associates with brain atrophy, whereas glial fibrillary acidic protein (GFAP) is a marker of astrocytic activation, associated with several neurodegenerative diseases(37,38). In a previous study in a similar cohort of patients with obesity and healthy lean controls, we had shown that

Nfl associates inversely with brain density, although their circulating values seemed influenced by renal function(39).

Another notable finding was that group differences in ^{11}C-PK11195 uptake were confined to white matter. If higher ^{11}C-PK11195 uptake in lean subjects reflects better endothelial function, this observation is consistent with prior reports of white matter microvascular vulnerability in obesity. In diabetes, white matter microvasculature appears more susceptible than grey matter vasculature, as demonstrated by MRI and neuropathological studies. Proposed mechanisms include reduced perfusion, impaired capillary permeability, and BBB dysfunction, which contribute to the development of white matter hyperintensities commonly observed in patients with T2D. Hyperglycemia-driven pathways, such as increased advanced glycation endproduct (AGE) formation, protein kinase C activation, and polyol pathway flux, consume NADPH, reduce endothelial nitric oxide synthase (eNOS) activity, and impair nitric oxide production, leading to endothelial cell dysfunction. Although some participants with obesity in our study also had T2D, most were normoglycemic or had impaired glucose tolerance. Nevertheless, the pro-inflammatory *milieu* of obesity may promote oxidative stress and polyol pathway activation, contributing to endothelial cell dysfunction(40,41). Additionally, pro-inflammatory macrophages produce inducible nitric oxide synthase (iNOS), which, unlike eNOS, exacerbates chronic inflammation and endothelial injury. Associations between VAT and cerebral small vessel disease(42); as well as white matter microstructural alterations on diffusion tensor imaging (DTI), further support this intepretation(43). Of interest, we found associations between ^{11}C-PK11195 uptake and neurocognitive results only in patients with obesity but not in healthy controls. (..)

We have previously consistently demonstrated that in the context of an insulin clamp experiment, patients with obesity have enhanced BGU compared to healthy lean

controls(11,12). This finding was later confirmed in both human and animal studies, and we had shown that the strongest predictor of BGU under insulin clamp conditions is the degree of insulin sensitivity(20). The exact mechanisms behind this enhanced BGU – observed only during insulin stimulation and not under fasting conditions(44), remain elusive. Astrocytes, the most abundant cell type in the human brain, are widely distributed throughout the CNS and are known to proliferate in response to inflammatory insults to protect neurons. Moreover, PET studies have demonstrated that the [^{18}F]FDG signal is largely driven by astrocytic glucose uptake(45), which according to the astrocyte-neuron lactate shuttle (ANLS) hypothesis, is converted to lactate and supplied to the neurons(14). Based on these observations, we had hypothesized that the increased BGU observed in obesity during insulin clamp conditions might be driven by central inflammation. However, in this study we observed no association between ^{11}C-PK11195 uptake and insulin-stimulated BGU. If ^{11}C-PK11195 uptake primarily reflects endothelial TSPO, rather than astrocytosis, this dissociation is expected. Endothelial cells rely predominantly on the insulin-independent glucose transporter GLUT1, and thus would not be expected to correlate with insulin-stimulated BGU. Future studies employing tracers that specifically depict astrocytosis such as ^{11}C-deuterium-L-deprenyl(46), in combination with [^{18}F]FDG PET during insulin clamp conditions, may help clarifying whether astrogliosis contribute to the increased BGU observed in obesity.

Strengths of this study include the comprehensive phenotypic characterization of participants, the combination of molecular brain imaging with gold-standard assessment of insulin resistance, detailed cognitive evaluation, and measurement of systemic inflammatory markers and the analysis of human brain samples to explain our clinical findings. Several limitations should also be acknowledged. The primary limitation relates to the intrinsic shortcomings of ^{11}C-PK11195, including high nonspecific binding and limited sensitivity for

detecting low-grade neuroinflammation in neurologically healthy individuals with obesity. Additionally, although a longitudinal follow-up study after metabolic bariatric surgery was originally planned, the unexpected initial ^{11}C-PK11195 PET findings led to discontinuation of PET imaging at 18 months. Given current insight, it would be highly informative to investigate whether ^{11}C-PK11195 uptake is enhanced following weight loss, possibly suggesting better white matter endothelial function, Regarding the biopsy analyses, we decided to analyse human brain tissue, only following the clinical study; thus the planning of these studies did not involve a thorough evaluation of brain inflammation, but rather tried to explain the clinical findings. For this reason, only white matter sections were analysed, as the ^{11}C-PK11195 uptake was different between the two groups in white matter. Despite this limitation, we found evidence of inflammation in the studied region. Future studies will be needed to assess whether there is direct evidence of brain inflammation in humans in other important brain areas, such as the prefrontal cortex, the hypothalamus, and the limbic system. Moreover, the use of limited phenotypic markers (CD68 and CD31) may not fully capture cellular heterogeneity. Furthermore, standard immunofluorescence microscopy constrains resolution and three-dimensional interpretation, limiting detection of subtle co-localization differences. Future studies using higher-resolution techniques, such as confocal microscopy or spatial multi-omics approaches could provide deeper insight into TSPO expression across cellular compartments.

In conclusion, we show for the first time definite evidence of white matter inflammation in the context of human obesity. More research is needed to define whether inflammation occurs also in other brain regions. Our study also unravels for the first time a novel – thus far undefined role of ^{11}C-PK11195 PET imaging to depict endothelial function; the clinical applications of this finding could be huge, but first confirmatory studies are

needed. Finally, the mechanisms underlying increased brain glucose uptake in the context of systemic insulin resistance remain to be elucidated.

Acknowledgments: The authors thank Sanna Himanen the study nurse, and the staff of the Turku PET Centre for performing the PET imaging. No potential conflicts of interest relevant to this article were reported.

Author's contribution: ER, MJH, ALR, ES, performed the studies. JT, analyzed the ^{11}C-PK11195 data and ^{18}F-FDG data. RA analyzed the ^{11}C-PK11195 metabolite data. PS, MH, SK recruited the obese patients and obtained the tissue samples. SP performed the analyses on brain samples. ER and PN conceived the study design. ER, LE, searched the literature and drafted the manuscript. LN, JR, AR, PN reviewed the manuscript. All authors approved the final version of the manuscript. PN is the guarantor of this work and, as such, had full access to all the data in the study and takes responsibility for the integrity of the data and the accuracy of the data analysis.

Funding: EFSD grant (PN); ER reports funding from the Emil Aaltonen Säätiö, Finnish Cultural Foundation, Paulon Säätiö, Paavo Nurmi Foundation, Finnish Diabetes research foumdation, Suomen Lääketieteen Säätiö.

Figure Legends

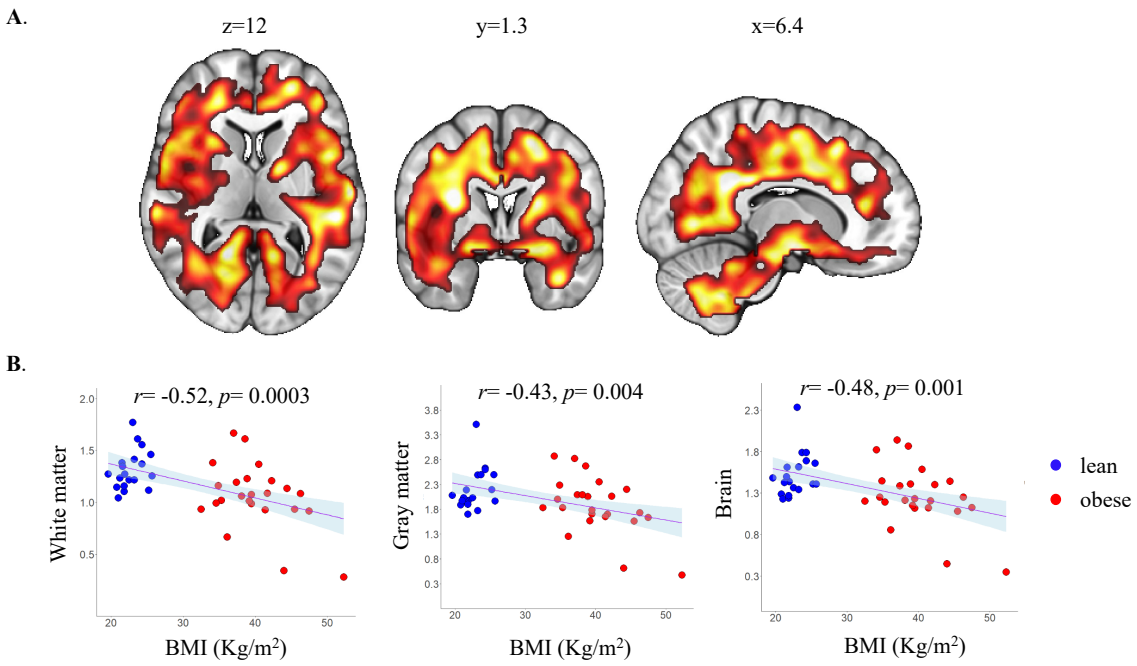

Figure 1- A, Statistical parametric mapping (SPM) two-sample t test between patients with obesity and heathly lean controls. Marked brain areas show regions with significantly higher TSPO availability in healthy lean controls compared compared to patients with obesity. Higher T values denote larger differences between groups. P values <0.05 cluster level, false discovery rate (FDR)-corrected. **B**, Inverse association between TSPO availability and body mass index. For visualization purposes the white matter, gray matter and whole brain regions of interest were extracted and used.

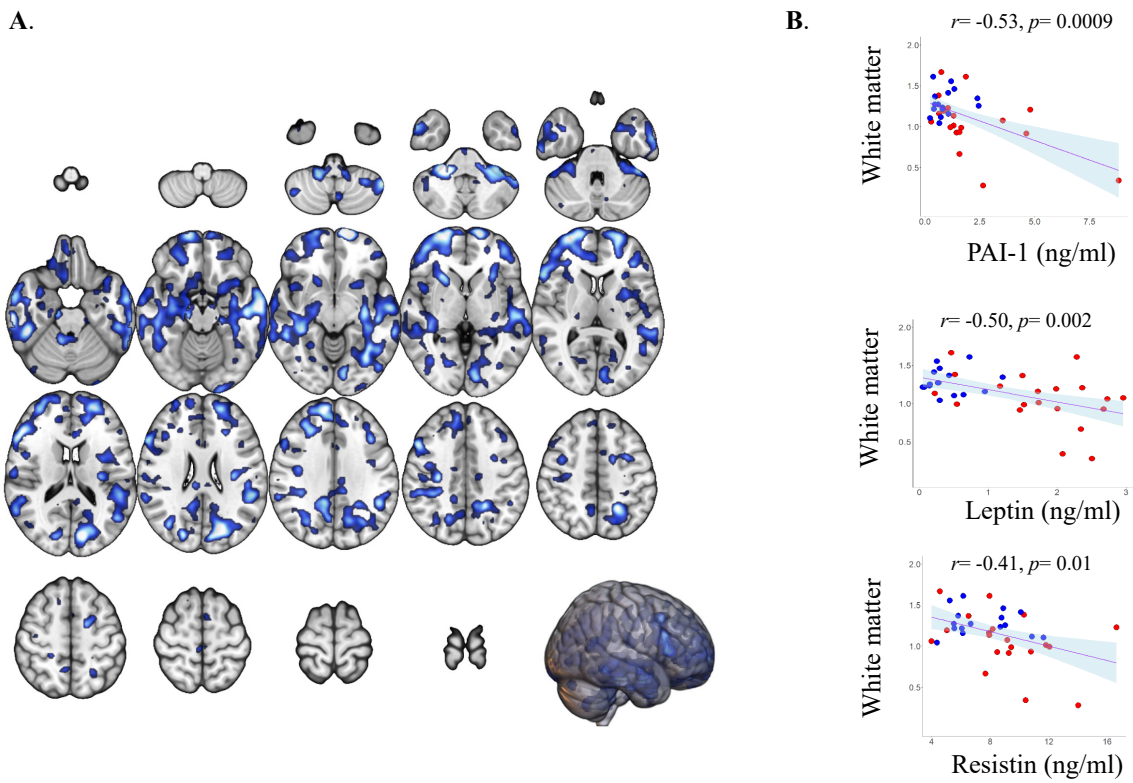

Figure 2-A) Statistical parametric mapping (SPM) one-sample t test for the inverse association between TSPO availability and circulating levels of PAI-1, among all subjects. Higher T values denote stronger association. P values <0.05 cluster level, false discovery rate (FDR)-corrected. **B**) Inverse association between TSPO availability using the extracted white matter ROI data and circulating PAI-1, leptin and resistin levels.

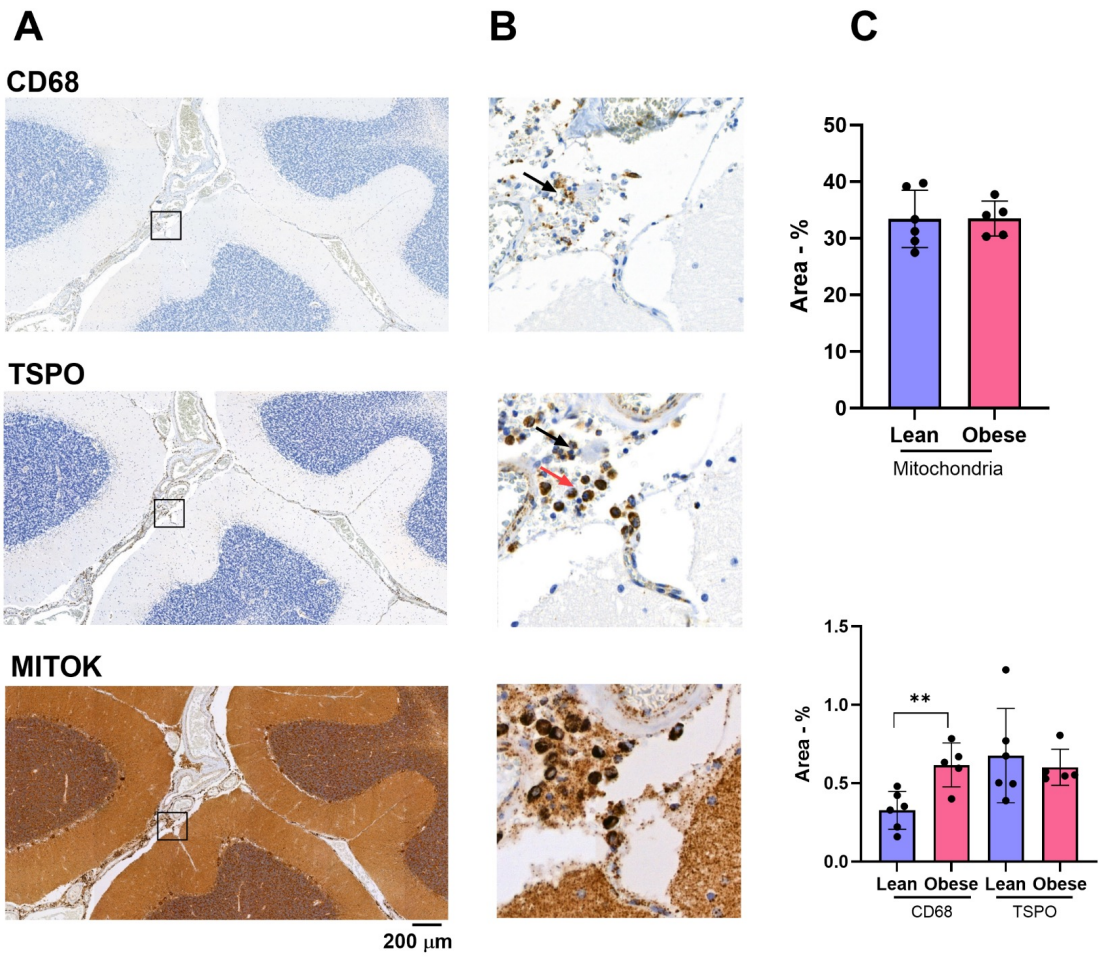

Figure 3- Immunostaining ob human brain tissue sections, **A**) Representative immunostainings on human brain tissue section with CD68, TSPO, and MITOK. **B**) Higher magnification black squares from images in A. **C**) Quantification of area% of MITOK, CD68 and TSPO, on lean donors and donors who had obesity. Scale bar = 200 µm.

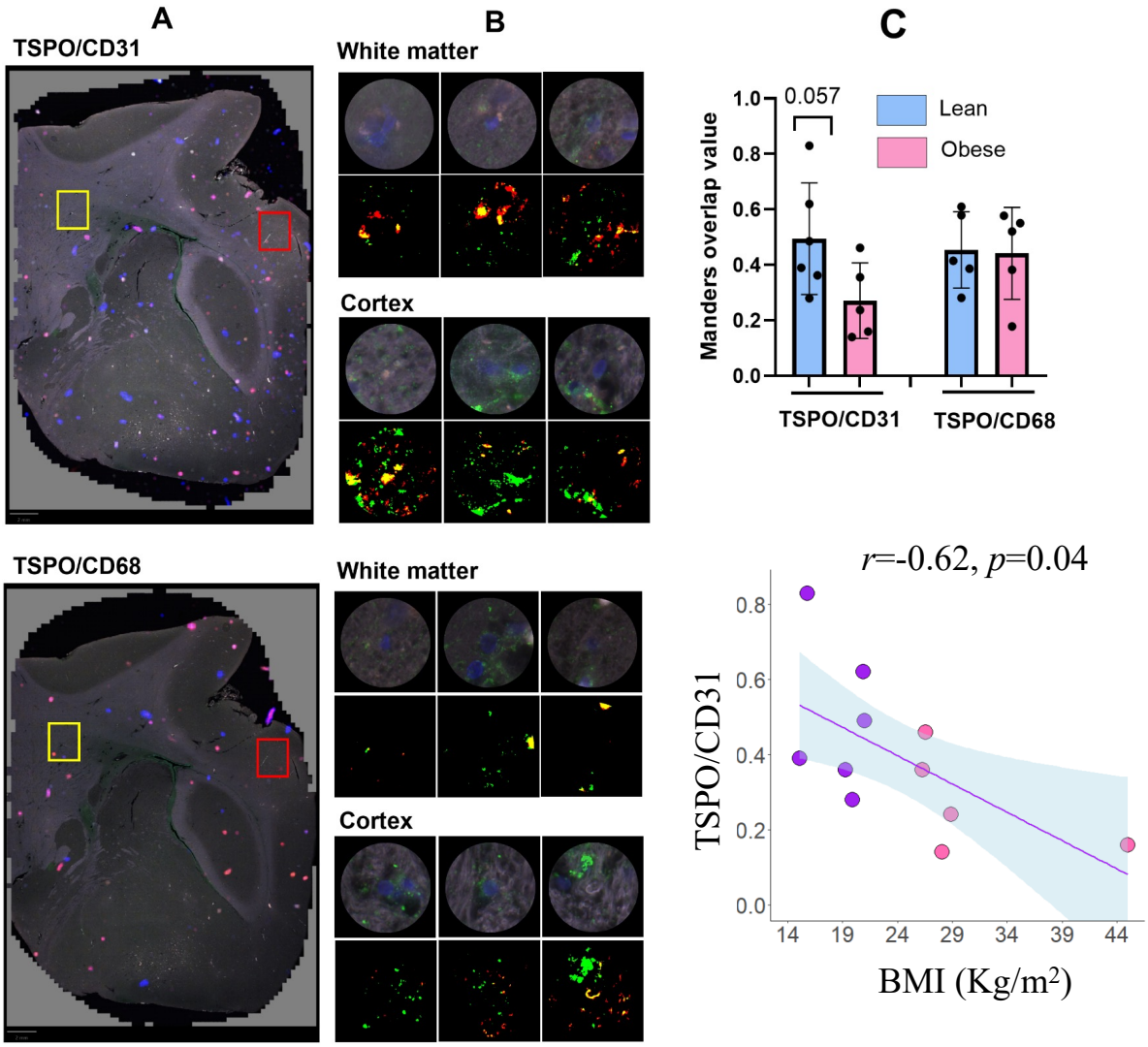

Figure 4- A) Immunofluorescent staining on same sections shows that CD31-positive endothelia are also positive for TSPO; CD68-positive macrophages are also positive for TSPO. **B**) Higher magnifications of the image analysis using Qupath, Yellow box – white matter, Red box – Cortex. **C**) Quantification of TSPO presence on endothelial cells and Macrophages from Lean and Obese. **D**) TSPO/CD31 was inversely related to BMI. Scale bar= 2 mm. Zoomed region scale bar = 39 µm.

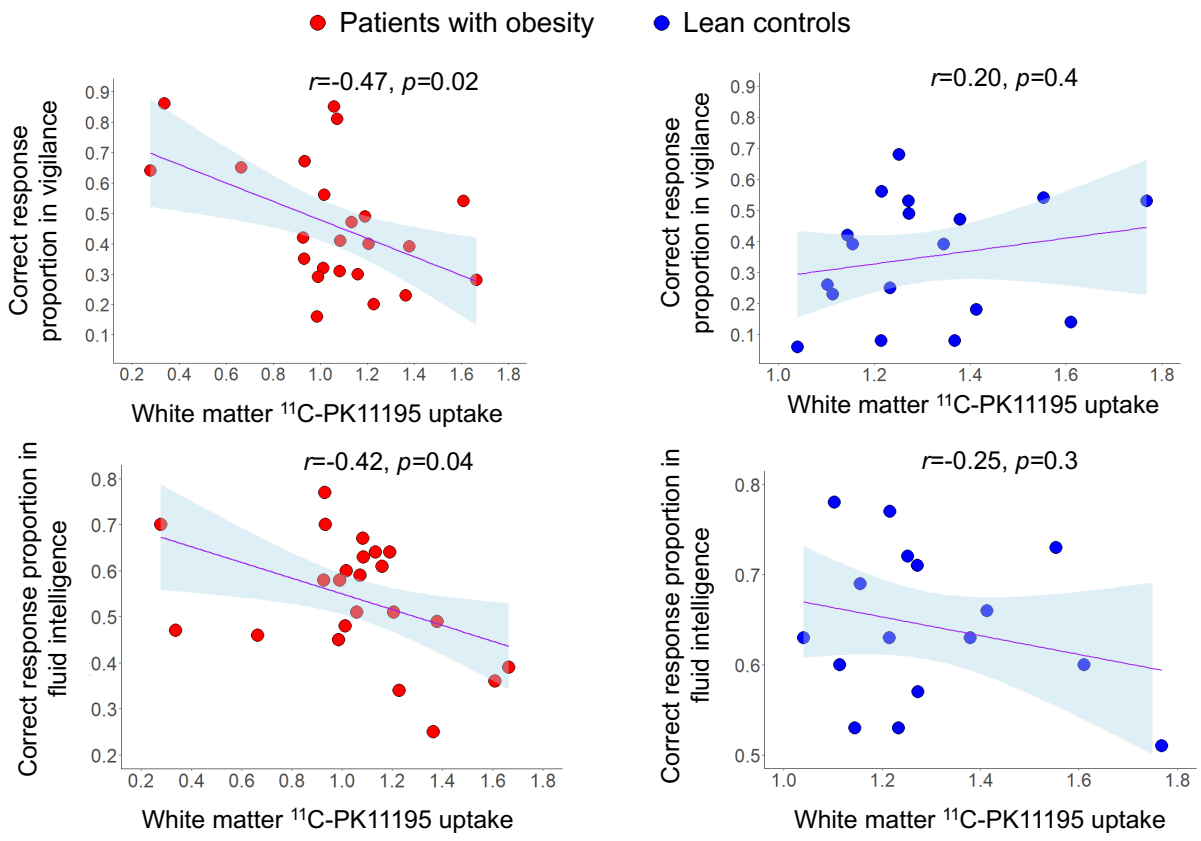

Figure 5- Correlations between neurocognitive test domains of vigilance and fluid intelligence with white matter ^{11}C-PK11195 uptake in the two groups.

References

1. Hotamisligil GS. Inflammation and metabolic disorders. Nature. 2006 Dec;444(7121):860–7.

2. Thaler JP, Guyenet SJ, Dorfman MD, Wisse BE, Schwartz MW. Hypothalamic inflammation: marker or mechanism of obesity pathogenesis? Diabetes. 2013 Aug;62(8):2629–34.

3. Thaler JP, Yi C-X, Schur EA, Guyenet SJ, Hwang BH, Dietrich MO, et al. Obesity is associated with hypothalamic injury in rodents and humans. J Clin Invest. 2012 Jan;122(1):153–62.

4. Schain M, Kreisl WC. Neuroinflammation in Neurodegenerative Disorders-a Review. Curr Neurol Neurosci Rep. 2017 Mar;17(3):25.

5. Pascoal TA, Benedet AL, Ashton NJ, Kang MS, Therriault J, Chamoun M, et al. Microglial activation and tau propagate jointly across Braak stages. Nat Med. 2021 Sep;27(9):1592–9.

6. Yu ZB, Han SP, Cao XG, Guo XR. Intelligence in relation to obesity: a systematic review and meta-analysis. Obes Rev an Off J Int Assoc Study Obes. 2010 Sep;11(9):656–70.

7. Veronese N, Facchini S, Stubbs B, Luchini C, Solmi M, Manzato E, et al. Weight loss is associated with improvements in cognitive function among overweight and obese people: A systematic review and meta-analysis. Neurosci Biobehav Rev. 2017 Jan;72:87–94.

8. Rebelos E, Hirvonen J, Bucci M, Pekkarinen L, Nyman M, Hannukainen JC, et al. Brain free fatty acid uptake is elevated in morbid obesity, and is irreversible 6 months after bariatric surgery: A positron emission tomography study. Diabetes Obes Metab. 2020 Jul;22(7):1074–82.

9. Schur EA, Melhorn SJ, Oh S-K, Lacy JM, Berkseth KE, Guyenet SJ, et al. Radiologic evidence that hypothalamic gliosis is associated with obesity and insulin resistance in humans. Obesity (Silver Spring). 2015 Nov;23(11):2142–8.

10. Lee D, Thaler JP, Berkseth KE, Melhorn SJ, Schwartz MW, Schur EA. Longer T(2) relaxation time is a marker of hypothalamic gliosis in mice with diet-induced obesity. Am J Physiol Endocrinol Metab. 2013 Jun;304(11):E1245-50.

11. Tuulari JJ, Karlsson HK, Hirvonen J, Hannukainen JC, Bucci M, Helmiö M, et al. Weight loss after bariatric surgery reverses insulin-induced increases in brain glucose metabolism of the morbidly obese. Diabetes. 2013 Aug;62(8):2747–51.

12. Rebelos E, Immonen H, Bucci M, Hannukainen JC, Nummenmaa L, Honka M-J, et al. Brain glucose uptake is associated with endogenous glucose production in obese patients before and after bariatric surgery and predicts metabolic outcome at follow-up. Diabetes Obes Metab. 2019 Feb;21(2):218–26.

13. Boersma GJ, Johansson E, Pereira MJ, Heurling K, Skrtic S, Lau J, et al. Altered Glucose Uptake in Muscle, Visceral Adipose Tissue, and Brain Predict Whole-Body Insulin Resistance and may Contribute to the Development of Type 2 Diabetes: A Combined PET/MR Study. Horm Metab Res = Horm und Stoffwechselforsch = Horm Metab. 2018 Aug;50(8):627–39.

14. Pellerin L, Magistretti PJ. Glutamate uptake into astrocytes stimulates aerobic glycolysis: a mechanism coupling neuronal activity to glucose utilization. Proc Natl Acad Sci U S A. 1994 Oct;91(22):10625–9.

15. 2. Classification and Diagnosis of Diabetes: Standards of Medical Care in Diabetes-2019. Diabetes Care. 2019 Jan;42(Suppl 1):S13–28.

16. DeFronzo RA, Tobin JD, Andres R. Glucose clamp technique: a method for quantifying insulin

secretion and resistance. Am J Physiol. 1979 Sep;237(3):E214-23.

17. Rebelos E, Honka M-J. PREDIM index: a useful tool for the application of the euglycemic hyperinsulinemic clamp. J Endocrinol Invest. 2020 Jul;

18. Karjalainen T, Tuisku J, Santavirta S, Kantonen T, Bucci M, Tuominen L, et al. Magia: Robust Automated Image Processing and Kinetic Modeling Toolbox for PET Neuroinformatics. Front Neuroinform. 2020;14:3.

19. Schubert J, Tonietto M, Turkheimer F, Zanotti-Fregonara P, Veronese M. Supervised clustering for TSPO PET imaging. Eur J Nucl Med Mol Imaging. 2021 Dec;49(1):257–68.

20. Rebelos E, Bucci M, Karjalainen T, Oikonen V, Alessandra, Bertoldo, Hannukainen JC, et al. Insulin resistance is associated with enhanced brain glucose uptake during euglycemic hyperinsulinemia: A large-scale PET cohort. Diabetes Care. 2021;44:1–7.

21. Wu H-M, Bergsneider M, Glenn TC, Yeh E, Hovda DA, Phelps ME, et al. Measurement of the global lumped constant for 2-deoxy-2-[18F]fluoro-D-glucose in normal human brain using [15O]water and 2-deoxy-2-[18F]fluoro-D-glucose positron emission tomography imaging. A method with validation based on multiple methodologies. Mol imaging Biol. 2003;5(1):32–41.

22. Gastaldelli A, Casolaro A, Pettiti M, Nannipieri M, Ciociaro D, Frascerra S, et al. Effect of pioglitazone on the metabolic and hormonal response to a mixed meal in type II diabetes. Clin Pharmacol Ther. 2007 Feb;81(2):205–12.

23. Anwyl-Irvine AL, Massonnié J, Flitton A, Kirkham N, Evershed JK. Gorilla in our midst: An online behavioral experiment builder. Behav Res Methods. 2020 Feb;52(1):388–407.

24. Chierchia G, Fuhrmann D, Knoll LJ, Pi-Sunyer BP, Sakhardande AL, Blakemore S-J. The matrix reasoning item bank (MaRs-IB): novel, open-access abstract reasoning items for adolescents and adults. R Soc open Sci. 2019 Oct;6(10):190232.

25. Lang PJ, Greenwald MK, Bradley MM, Hamm AO. Looking at pictures: affective, facial, visceral, and behavioral reactions. Psychophysiology. 1993 May;30(3):261–73.

26. Spyridaki EC, Simos P, Avgoustinaki PD, Dermitzaki E, Venihaki M, Bardos AN, et al. The association between obesity and fluid intelligence impairment is mediated by chronic low-grade inflammation. Br J Nutr. 2014 Nov;112(10):1724–34.

27. Gunstad J, Paul RH, Cohen RA, Tate DF, Gordon E. Obesity is associated with memory deficits in young and middle-aged adults. Eat Weight Disord. 2006 Mar;11(1):e15-9.

28. Gunstad J, Paul RH, Cohen RA, Tate DF, Spitznagel MB, Gordon E. Elevated body mass index is associated with executive dysfunction in otherwise healthy adults. Compr Psychiatry. 2007;48(1):57–61.

29. Brogan A, Hevey D, O'Callaghan G, Yoder R, O'Shea D. Impaired decision making among morbidly obese adults. J Psychosom Res. 2011 Feb;70(2):189–96.

30. Betlazar C, Harrison-Brown M, Middleton RJ, Banati R, Liu G-J. Cellular Sources and Regional Variations in the Expression of the Neuroinflammatory Marker Translocator Protein (TSPO) in the Normal Brain. Int J Mol Sci. 2018 Sep;19(9).

31. Lupu F, Bergonzelli GE, Heim DA, Cousin E, Genton CY, Bachmann F, et al. Localization and production of plasminogen activator inhibitor-1 in human healthy and atherosclerotic arteries. Arterioscler Thromb a J Vasc Biol. 1993 Jul;13(7):1090–100.

32. Versijpt J, Debruyne JC, Van Laere KJ, De Vos F, Keppens J, Strijckmans K, et al. Microglial

imaging with positron emission tomography and atrophy measurements with magnetic resonance imaging in multiple sclerosis: a correlative study. Mult Scler. 2005 Apr;11(2):127–34.

33. Hentilä J, Tuisku J, Ojala R, Sun L, Lietzén MS, Virtanen H, et al. Obesity is associated with increased brain glucose uptake and activity but not neuroinflammation (TSPO availability) in monozygotic twin pairs discordant for BMI-Exercise training reverses increased brain activity. Diabetes Obes Metab. 2025 Dec;27(12):7097–109.

34. Tuisku J, Plavén-Sigray P, Gaiser EC, Airas L, Al-Abdulrasul H, Brück A, et al. Effects of age, BMI and sex on the glial cell marker TSPO - a multicentre [(11)C]PBR28 HRRT PET study. Eur J Nucl Med Mol Imaging. 2019 Oct;46(11):2329–38.

35. Alessi MC, Peiretti F, Morange P, Henry M, Nalbone G, Juhan-Vague I. Production of plasminogen activator inhibitor 1 by human adipose tissue: possible link between visceral fat accumulation and vascular disease. Diabetes. 1997 May;46(5):860–7.

36. Eriksson P, Reynisdottir S, Lönnqvist F, Stemme V, Hamsten A, Arner P. Adipose tissue secretion of plasminogen activator inhibitor-1 in non-obese and obese individuals. Diabetologia. 1998 Jan;41(1):65–71.

37. Lewczuk P, Ermann N, Andreasson U, Schultheis C, Podhorna J, Spitzer P, et al. Plasma neurofilament light as a potential biomarker of neurodegeneration in Alzheimer's disease. Alzheimers Res Ther. 2018 Jul;10(1):71.

38. Lafrenaye AD, Mondello S, Wang KK, Yang Z, Povlishock JT, Gorse K, et al. Circulating GFAP and Iba-1 levels are associated with pathophysiological sequelae in the thalamus in a pig model of mild TBI. Sci Rep. 2020 Aug;10(1):13369.

39. Rebelos E, Rissanen E, Bucci M, Jääskeläinen O, Honka M-J, Nummenmaa L, et al. Circulating neurofilament is linked with morbid obesity, renal function, and brain density. Sci Rep. 2022 May;12(1):7841.

40. Čolak E, Pap D. The role of oxidative stress in the development of obesity and obesity-related metabolic disorders. J Med Biochem. 2021 Jan;40(1):1–9.

41. Dandona P, Ghanim H, Chaudhuri A, Dhindsa S, Kim SS. Macronutrient intake induces oxidative and inflammatory stress: potential relevance to atherosclerosis and insulin resistance. Exp Mol Med. 2010 Apr;42(4):245–53.

42. Kim KW, Seo H, Kwak M-S, Kim D. Visceral obesity is associated with white matter hyperintensity and lacunar infarct. Int J Obes (Lond). 2017 May;41(5):683–8.

43. Kullmann S, Callaghan MF, Heni M, Weiskopf N, Scheffler K, Häring H-U, et al. Specific white matter tissue microstructure changes associated with obesity. Neuroimage. 2016 Jan;125:36–44.

44. Jensen NJ, Porse AJ, Wodschow HZ, Speyer H, Krogh J, Marner L, et al. Relation of Insulin Resistance to Brain Glucose Metabolism in Fasting and Hyperinsulinemic States: A Systematic Review and Meta-Analysis. J Clin Endocrinol Metab. 2024 Aug;

45. Zimmer ER, Parent MJ, Souza DG, Leuzy A, Lecrux C, Kim H-I, et al. [(18)F]FDG PET signal is driven by astroglial glutamate transport. Nat Neurosci. 2017 Mar;20(3):393–5.

46. Carter SF, Schöll M, Almkvist O, Wall A, Engler H, Långström B, et al. Evidence for astrocytosis in prodromal Alzheimer disease provided by 11C-deuterium-L-deprenyl: a multitracer PET paradigm combining 11C-Pittsburgh compound B and 18F-FDG. J Nucl Med. 2012

Jan;53(1):37–46.

Table 1 – Anthropometric and biochemical characteristics of the study participants*.

	Lean	**Obese**	***p* value**
M/W	4/15	5/19	ns
Age (years)	48 [22]	49 [17]	ns
BMI ($Kg \cdot m^{-2}$)	22.5 [2.8]	39.4 [7.3]	<0.0001
Waist/Hip	0.80 [0.13]	0.91 [0.17]	<0.0001
NGT/IFG&IGT/T2D	16/3/0	9/11/4	0.007
HbA_{1c} (mmol/mol)	34 [4]	36 [6]	0.04
M value ($\mu mol/Kg_{FFM}/min$)	88.7 [44.5]	38.4 [30.8]	<0.0001
Total eGFR (ml/min)	93 ± 16	118 ± 23	0.0003
Plasma glucose (mmol/L)	5.0 [0.4]	5.6 [0.8]	0.0008
Plasma insulin (pmol/L)	35 ± 16	121 ± 57	<0.0001
Systolic BP (mmHg)	120 ± 11	139 ± 13	<0.0001
Diastolic BP (mmHg)	78 ± 8	85 ± 8	0.007
Total cholesterol (mmol/L)	4.4 ± 0.9	4.4 ± 0.8	ns
LDL cholesterol (mmol/L)	2.6 ± 0.8	2.7 ± 0.6	ns
HDL cholesterol (mmol/L)	1.6 ± 0.4	1.2 ± 0.2	0.0005
Triglycerides (mmol/L)	0.8 [0.4]	1.2 [0.5]	0.0003
C-reactive protein (mg/dL)	0.6 [0.6]	3.4 [3.4]	<0.0001
Leptin (pg/ml)	296 [211-638]	1859 [1241-2357]	<0.0001
TNF-a (pg/ml)	1.31 [1.05-1.58]	1.74 [1.28-2.31]	0.02
Adiponectin (pg/ml)	55209 [28586-84983]	51549 [35792-63121]	0.7
PAI-1 (pg/ml)	765 [458-1166]	1377 [774-2452]	0.02
NfL (ng/L)	11.5 [7.4-14.6]	11.2 [8.6-16.7]	0.5
GFAP (ng/L)	84.2 [57.3-126.3]	85.3 [55.3-117.0]	>0.9

*entries are mean±SD, or median [IQR] as appropriate.

Table 2 – Cognitive function tests

	Lean	**Obese**	***p* value**
Cerad – Learning (%) correct answers	69 [59-83]	63 [57-73]	0.3
Vigilance (%) correct answers	39 [17-53]	41 [30-64]	0.1
2-back (%) correct answers	90 [88-95]	83 [78-89]	**0.001**
2-back mean reaction time (ms)	760 [642-822]	689 [556-854]	0.1
Simple reaction time: mean reaction time (ms)	391 [341-449]	368 [359-411]	0.9
Word span (maximum)	88 [75-91]	88 [75-88]	>0.9
Fluid intelligence (%) correct answers	63 [53-71]	58 [46-64]	**0.03**
Cerad – Delayed free recall (%) correct answers	60 [40-90]	60 [50-73]	0.6
Cerad – Delayed cued recall % correct answers	100 [90-100]	95 [90-100]	0.3

*entries are median [IQR] as appropriate.